Int. J. Heat Mass Transfer. Vol. 31, No. 2, pp. 311–319, 1988
Printed in Great Britain

0017-9310/88 $3.00 + 0.00

Analytical study of the structure of radiation controlled flame

YOSHIO YOSHIZAWA, KIYOSHI SASAKI and RYOZO ECHIGO
Department of Mechanical Engineering, Tokyo Institute of Technology, Tokyo 152, Japan

(*Received* 31 *August* 1987)

Abstract—This study is aimed at clarifying the effects of radiative heat transfer on the flame structure and burning velocity in gas–solid two-phase systems. Based on a strict treatment of radiation, a detailed numerical analysis has been performed for a one-dimensional model of premixed combustion in a porous medium, and the effects of the absorption coefficient and total optical thickness of the porous medium, as well as the position of the reaction zone within the porous medium on the flame structures and burning velocity have been elucidated.

1. INTRODUCTION

THE AUTHORS have shown in a previous work [1] that a porous medium of an appropriate optical thickness placed in a duct can be very effective in converting the sensible enthalpy of a flowing gas to thermal radiation directed toward the higher temperature side. The authors have also reported on successful applications of this phenomenon for combustion augmentation of extremely low calorific gases [2] and for radiative heat transfer enhancement [3]. The thermal structures (profiles of temperature, radiant energy density, etc.) in porous media with internal heat generation have also been studied experimentally as well as analytically, and the mechanisms of combustion augmentation and heat transfer enhancement have been clarified [4]. The energy feedback by radiant heat exchange across the reaction zone causes combustion augmentation. The radiation shielding and extremely high radiant energy density in the prescribed space provide intense radiant heat transfer. However, for more sophisticated engineering applications, the structure of radiation controlled flames needs to be understood in considerable detail.

The general recognition of the importance of radiation on the combustion of gas–solid two-phase systems such as pulverized coal combustion [5] and large-scale combustion phenomena in fire [6] and industrial furnaces [7] has resulted in numerous publications. Nevertheless, almost all the literature gives only specific answers to a variety of technological problems of urgent need, and only a few studies have focused on fundamental concepts such as the effects on flame structure and burning velocity [8–10]. Arpaci and Tabaczynski [8] have reported the effects of radiation on laminar flame thickness, in which some dimensionless numbers have been introduced. However, the mathematics of radiative transfer are simplified by a differential formulation, and the effects of boundaries are ignored by considering a semi-infinite system, such that the results are rather qualitative. Joulin and Deshaies [9] have studied the effects of radiation on laminar flame speed, employing asymptotic techniques, and have pointed out an important characteristic, namely: the radiative preheating of unburnt mixture. However, they assumed that the radiative transfer contributed in only a small way to the energy equation, and that the radiant flux was able to be computed from the radiation-free, unperturbed temperature profile. They also assumed the system to be semi-infinite. Unlike an ordinary premixed gas-phase flame analysis in which the conduction and convection control the phenomena, and in which a system of practical size can be approximated as semi-infinite, a semi-infinite system in radiation analysis implies an optically thick system. Yuen and Zhu [10] have also reported the effects of radiation on the propagation of laminar flames in mixtures of small particles and gas. Although radiative heat transfer was formulated exactly and the resultant integral–differential equation was treated, they used the integral method without solving the temperature profile, and they assumed an inadequate temperature profile based on an incorrect prejudice, i.e. the temperature did not exceed the theoretical flame temperature. But as it is demonstrated in this work, as well as in previous works [2, 4], the radiative transfer builds up an energy feedback across the reaction zone causing excess enthalpy burning [11], which is one of the most important characteristics of radiation controlled flames, because it is the mechanism which increases the flame speed in gas–solid two-phase systems. Takeno and Hase have tried to explain excess enthalpy burning in gas–solid two-phase systems by heat conduction in the solid phase in their series of theoretical studies [12]. Since they assumed the solid phase temperature to be constant along the flow direction and ignored radiation heat transfer, their analysis was only applicable for an extremely thin porous solid. Nevertheless, the temperature profile in the combustor in their experimental study [13] shows that most preheating of the unburned gas takes place outside the thin flame zone, and it

NOMENCLATURE

A frequency factor in reaction rate [s^{-1}]
A_p surface area of an equivalent particle [m^2]
c specific heat at constant pressure [$J\ kg^{-1}\ K^{-1}$]
D diffusion coefficient [$m^2\ s^{-1}$]
d_p diameter of an equivalent particle [m]
E activation energy in reaction rate constant [$J\ mol^{-1}$]
E_n exponential integral function of nth order, equation (8)
H dimensionless energy flux, equation (11)
h^0 heat of reaction [$J\ kg^{-1}$]
h_p heat transfer coefficient around an equivalent particle [$W\ m^{-2}\ K^{-1}$]
I_b total emissive power of a blackbody, equation (7) [$W\ m^{-2}$]
m mass flux (mass burning velocity) [$kg\ m^{-2}\ s^{-1}$]
n_p number density of equivalent particles [m^{-3}]
q_R^+, q_R^-, q_R^n radiative heat fluxes toward positive and negative directions and net radiative heat flux, respectively [$W\ m^{-2}$]
R incident radiance to both ends of the porous medium [$W\ m^{-2}$]
R_g gas constant, 8.314 $J\ mol^{-1}\ K^{-1}$
S_u burning velocity [$m\ s^{-1}$]
T temperature [K]
T_b adiabatic flame temperature [K]
t time [s]
u velocity of gas phase [$m\ s^{-1}$]
W mass production rate of the product species [$kg\ m^{-3}$]
x geometrical coordinate system (Fig. 1) [m]
y mass fluction of the product species.

Greek symbols
α thermal diffusivity [$m^2\ s^{-1}$]
2δ thickness of region (II) (Fig. 1) where the combustion reaction is taken into account [m]
Δ flame thickness [m]
κ absorption coefficient [m^{-1}]
λ thermal conductivity [$W\ m^{-1}\ K^{-1}$]
ρ density [$kg\ m^{-3}$]
σ Stefan–Boltzmann constant, 56.7 $nW\ m^{-2}\ K^{-4}$
τ optical coordinate system, κx (Fig. 1).

$H_R, J, K, M, N_R, N_u, \beta, \Gamma, \theta, \chi$ dimensionless quantities, equation (10).

Subscripts
0, f, e coordinate (Fig. 1) (0 is also used to denote the values of the flame in the gas phase)
p particulate phase (subscript for the gas phase is omitted).

demonstrates the importance of radiation heat transfer across the flame zone.

The present study analyzes a premixed flame in a porous medium; and the effects of radiative heat transfer on flame structure and burning velocity are clarified by a rigorous treatment of radiation.

2. NUMERICAL ANALYSIS

2.1. *Analytical model*

A one-dimensional model is shown in Fig. 1. The thickness of the porous medium is assumed to have a physical length, x_e, and an optical length, τ_e. A combustible gas mixture having an initial temperature T_0 flows into the porous medium at $x = 0$, burns in the neighborhood $x = x_f$ and flows out of the other end of the porous medium ($x = x_e$) at temperature T_e. The porous medium is divided into three regions for numerical analysis. Regions I and III are considered inert and the combustion reaction is assumed to take place entirely in region II. A sufficient thickness, 2δ, is allocated to region II. Both ends of the porous medium are exposed to blackbody surfaces at ambient temperature T_0 providing incident radiance R_0 and R_e, respectively, while the ends have radiation heat losses q_{R0}^- and q_{Re}^+, respectively. Denoting the mass burning velocity of the system by $m = \rho u$, the flame is stabilized for some range of m, and the position of the flame moves correspondingly. The typical assumption that the burnt gas temperature can be equated to the adiabatic flame temperature is not applicable to this system because of the presence of radiative heat loss and incident radiation, as well as the onset of energy feed back across the reaction zone.

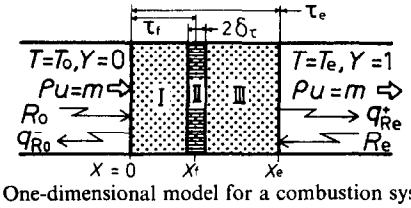

FIG. 1. One-dimensional model for a combustion system in a porous medium.

The assumptions invoked for radiation heat transfer are similar to those of previous works [1, 4]. The principal assumptions are as follows:

(a) the working gas is non-radiating;
(b) the porous medium consists of fine solid particles dispersed homogeneously;
(c) the porous medium is able to emit and absorb

thermal radiation in local thermal equilibrium, while radiative scattering is ignored;

(d) a one-dimensional approximation of radiative propagation along the x-direction is assumed;

(e) the physical properties are constant.

The assumptions for the reaction system are:

(f) the porous medium is non-catalytic;

(g) both the reduction in the cross-section and the pressure drop caused by the presence of the porous medium are ignored; gas flow is assumed to be sufficiently slow for the process to remain isobaric;

(h) the combustion reaction is described by an irreversible first-order isomerization, $R \rightarrow P$.

(i) The Lewis number is unity.

In addition to these assumptions, those assumptions usually employed in models of premixed flames [14] are also included here. Considering the appropriateness of these assumptions, assumption (a) is accurate because the emittance of the solid phase is far larger than that of the gas phase. Assumption (b) requires that the particles be small in comparison with the flame thickness and have a sufficiently high number density to be homogeneous within the medium. Assumption (c) is reasonable for metallic porous media with oxidized surfaces such as those employed in previous works [1–4], but it is not adequate for some materials [15]. Therefore, this assumption, as well as assumption (f), depends on the nature of the solid phase. Assumption (d) is easily realized by simple thermal insulation of the outer surface of the duct, since radial flow is not present and the radial temperature gradient is far smaller than the axial gradient. Assumptions (e), (g), (h) and (i) do not change the essential nature of the phenomenon and are only included here for simplicity and to save computational time. However, it is not difficult to remove these latter restrictions. A calculation was performed in which the variations of physical properties were taken into account, and it was confirmed that the effects on the flame structures were small because of the extremely high heat transfer coefficient and large surface area of the porous media.

2.2. *Basic equations*

Although the system eventually reaches a steady-state condition, the transient Spalding procedure [16] was used to numerically solve the time-dependent flame equations. Using the preceding assumptions, the energy equations for both the gas and particulate phases, as well as the continuity equation for species are formulated, respectively, as

$$\rho c\frac{\partial T}{\partial t}+\rho cu\frac{\partial T}{\partial x}=\lambda\frac{\partial^2 T}{\partial x^2}+\{Wh^0\}-h_p n_p A_p(T-T_p) \tag{1}$$

$$\rho_p c_p\frac{\partial T_p}{\partial t}=\lambda_p\frac{\partial^2 T_p}{\partial x^2}-\frac{\partial q_R}{\partial x}+h_p n_p A_p(T-T_p) \tag{2}$$

$$\rho\frac{\partial y}{\partial t}+\rho u\frac{\partial y}{\partial x}=D\rho\frac{\partial^2 y}{\partial x^2}+\{W\}. \tag{3}$$

The last terms in equations (1) and (2) express the heat exchange between the gas and particulate phases. The terms in braces in equations (1) and (3) describe the combustion reaction taking place in region II only. This model can be easily extended to a system containing the flowing and/or reactive solid phase if a convection term and/or a reaction term are added to equation (2), which have been omitted since the solid phase is assumed to be stationary and inert in this study. The reaction rate, W, is considered to obey the first-order Arrhenius equation

$$W=A\rho(1-y)\exp(-E/R_g T). \tag{4}$$

The mass burning rate, m, is computed by integration of the net mass production of product species throughout the system

$$m=\rho_0 S_u=\rho u=\int_{-\infty}^{\infty} W\,\mathrm{d}x=\int_{x_f-\delta}^{x_f+\delta} W\,\mathrm{d}x. \tag{5}$$

It is not assumed constant during the process of computation; instead, the approximate flame position is assumed fixed during each computation. The radiant flux from each part of the porous medium is integrated to evaluate the divergence of radiative heat flux by the following equation:

$$\frac{\partial q_R(\tau)}{\partial x}=-2\pi\kappa\Big[R_0E_2(\tau)+R_eE_2(\tau_e-\tau)-2I_b(\tau)+\int_0^{\tau} I_b(\tau')E_1(\tau-\tau')\,\mathrm{d}\tau'+\int_{\tau}^{\tau_e} I_b(\tau')E_1(\tau'-\tau)\,\mathrm{d}\tau'\Big] \tag{6}$$

where $I_b(\tau)$ and $E_n(\tau)$ are expressed as

$$I_b(\tau)=\sigma T_p^4/\pi \tag{7}$$

$$E_n(\tau)=\int_0^1 \mu^{n-2}\exp(-\tau/\mu)\,\mathrm{d}\mu. \tag{8}$$

The boundary conditions at $x=0$, $x=x_f\pm\delta$ and $x=x_e$ are

$$x=0\rightarrow T=T_0,\quad q_R^+=\pi R_0;\quad x=x_e\rightarrow q_R^-=\pi R_e;$$

$$x=x_f-\delta\rightarrow y=0;\quad x=x_f+\delta\rightarrow y=1. \tag{9}$$

These equations are then transformed into dimensionless form. The principal dimensionless variables and parameters are defined as

$$\chi=\frac{x}{x_e},\quad \beta=\frac{\alpha t}{x_e^2},\quad \theta=\frac{T-T_0}{T_b-T_0},\quad \theta_p=\frac{T_p-T_0}{T_b-T_0},$$

$$N_u=\frac{h_p d_p}{\lambda},\quad K=\frac{\lambda_p}{\lambda},\quad \Gamma=\frac{\rho_p c_p}{\rho c},\quad M=\frac{N_u n_p A_p x_e^2}{d_p},$$

$$N_R=\frac{\kappa\lambda}{4\sigma T_0^3},\quad H_R=\frac{q_R}{4\sigma T_0^4},\quad J=\frac{\pi R}{\sigma T_0^4}. \tag{10}$$

The overall energy balance of the system is expressed

by

$$H_1-(H_2+H_3+H_4)=1-(H_2+H_3+H_4)=0 \quad (11)$$

where H_1, H_2, H_3 and H_4 are, respectively, the total heat release rate, the sensible enthalpy flux exiting at the down-stream end and the radiation heat losses from the up- and down-stream ends all normalized by the total heat release rate. It is confirmed in a previous work [4] that other energy flows such as the heat conduction at both ends of the porous medium are negligible.

2.3. *Numerical method*

The conservation equations of species and energy are approximated by finite difference expressions where an implicit difference scheme is adopted with respect to time, and a central difference scheme is adopted with respect to space. More than 100 nodal points are employed both inside and outside of region II. In addition, non-uniform grid spacings are inserted on both sides of region II. The computation procedure is given below.

(1) Choose an approximate flame position, x_f, and a tentative thickness for region II, 2δ, where combustion can take place.

(2) Assume a mass flow rate, m, and initial distributions of temperatures, θ and θ_p, and concentration, y.

(3) Calculate the local chemical reaction rate, W, the mass burning velocity, m, and the divergence of radiative heat flux, $\partial q_R(\tau)/\partial x$ (equations (4)–(6)).

(4) Advance one time step and calculate the mass fraction, y, and the gas and particulate-phase temperatures, θ and θ_p, using an iterative procedure (equations (1)–(3)).

(5) Calculate the overall energy balance (equation (11)), and return to step (3) if it exceeds a preset value.

The initial temperature distributions were estimated using the method employed in a previous work [4] where the heat source was distributed uniformly in region II. On the other hand, the initial distribution of concentration was represented by a smooth curve. The profiles were checked every 100 time steps, and the appropriateness of δ was also judged at the same time. Since the mass burning velocity and the profiles of the temperatures and the mass fraction usually converge more rapidly than the overall energy balance, the overall energy balance is used to judge the overall convergence to a steady-state solution. The final error in the overall energy balance is usually less than 2%, but it occasionally exceeds 4%. It might appear to be coarse, but the greater part of it arises from the evaluation of the gradient of radiative heat flux because of the steep temperature profile in the porous medium. It was confirmed in a previous work [4] that this error was able to be reduced using smaller grid spacing. However, it requires considerable computational time.

The absorption coefficient κ, the optical thickness of the porous medium τ_e and the approximate position of the flame τ_f/τ_e are taken as given parameters in this calculation procedure. The numerical values of other important parameters employed for the computation are: the dimensionless parameter describing the heat transfer coefficient between gas and particles, $M=5\times10^4$, the ratio of thermal conductivities of gas and particulate phases, $K=1.0$, the ratio of heat capacities per unit volume $\Gamma=20$, the activation energy $E=130$ kJ mol^{-1}, the frequency factor $A=2.6\times10^8$ s^{-1} and the initial temperature $T_0=298$ K. Although the porous medium has a continuous structure in a practical system, it is usually difficult to estimate its absorption coefficient and heat transfer coefficient. Therefore, these parameters were evaluated on the basis of assumed spherical particles. On the other hand, the heat conduction in the porous medium was estimated on the basis of the volume fraction of the solid phase. Considering assumption (b), the diameter of the equivalent particles is assumed to be 20 μm. The values of E and A were selected such that the burning velocities calculated from these values coincided with those measured in methane–air mixtures at equivalence ratios $\phi=1.0$ and 0.52, and the heat of reaction was equated to a mixture having $\phi=0.5$. When considering the combustion of lean mixtures, the physical properties of the gas phase were taken for air at a temperature of 1273 K, except for the evaluation of burning velocity, which was taken as the mass burning velocity divided by the density at the initial temperature. Using these properties, the burning velocities and structures of ordinary gas-phase flames were computed using the same Spalding procedure [16], the result of which was used as the reference state, and the results for the two-phase system were normalized by these gas-phase flame values. The results for the ordinary gas-phase flame with $T_0=298$ K are as follows: $T_b=1478$ K, $S_{u0}=4.35$ cm s^{-1} and $\Delta_0=2.49$ mm. The local energy balance in this flame is shown later in Fig. 6.

3. RESULTS AND DISCUSSION

3.1. *Flame structures*

The computed results for parameters $\kappa=50$ m^{-1}, $\tau_e=2$ and $\tau_f/\tau_e=0.45$ are shown in Figs. 2 and 3. They

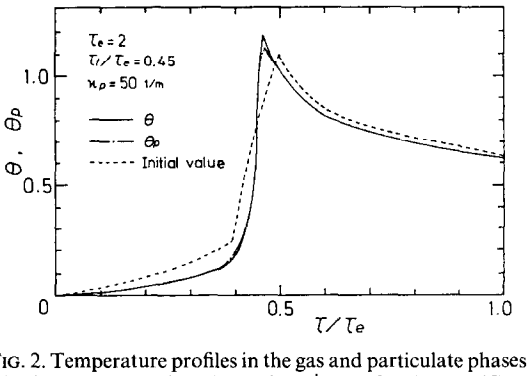

FIG. 2. Temperature profiles in the gas and particulate phases in the porous medium ($\kappa=50$ m^{-1}, $\tau_e=2$, $\tau_f/\tau_e=0.45$).

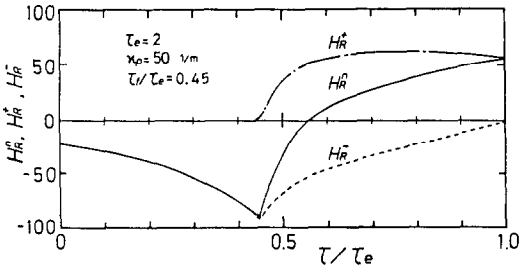

FIG. 3. Profiles of the radiant fluxes in the porous medium ($\kappa = 50\ m^{-1}$, $\tau_e = 2$, $\tau_f/\tau_e = 0.45$).

correspond to a system having a geometrical thickness of 4 cm, in which the reaction zone is 1.8 cm from the upstream end. The temperature profiles shown in Fig. 2 indicate that the temperature of the particulate phase is higher than that of the gas phase up to the reaction zone, and is lower afterwards, although the differences are very small except in the reaction zone. Magnified temperature profiles of region II are also shown in Fig. 5. The dotted line in Fig. 2 shows the initial values of the gas phase temperature used in the calculation. The net radiant flux, H_R^n, shown in Fig. 3 has large negative values around the reaction zone. These profiles of temperatures and radiant fluxes show a strong energy feedback across the reaction zone causing excess enthalpy burning, the concept of which was proposed by Weinberg [11]. The absolute values of H_R^n at both ends of the porous medium represent the radiation heat losses from the system, while the difference between the absolute values of the minimum in the reaction zone and that at the upstream end corresponds to the amount of energy feedback.

Figure 4 shows the local energy balance in the

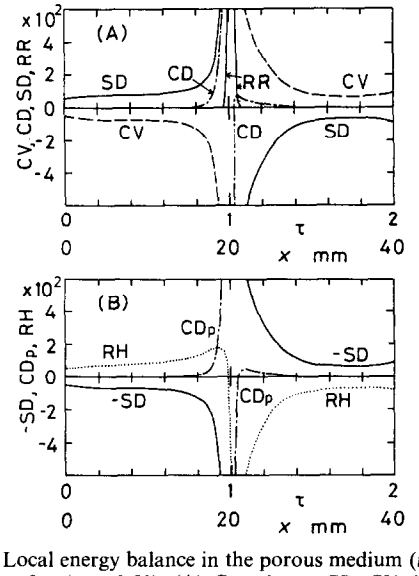

FIG. 4. Local energy balance in the porous medium ($\kappa = 50\ m^{-1}$, $\tau_e = 2$, $\tau_f/\tau_e = 0.50$). (A) Gas-phase; *CD*, *CV*, *SD* and *RR* are the dimensionless conductive, convective, inter-phase heat transfer and reaction rate energy terms, respectively. (B) Particulate phase; CD_p, $-SD$ and *RH* are the dimensionless conductive, inter-phase heat transfer and radiation energy terms, respectively.

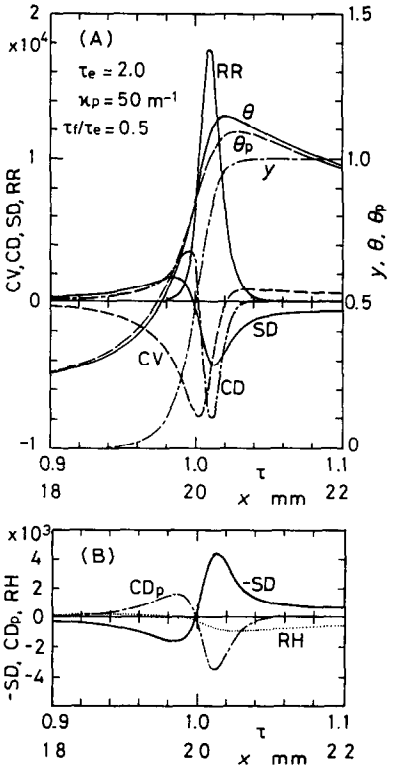

FIG. 5. Local energy balance in the reaction zone (the parameters and symbols are the same as those in Fig. 4).

porous medium and Fig. 5 shows its magnified profile in region II, where *CD*, *CV*, *SD* and *RR* represent the energy inputs (per unit dimensionless volume per unit dimensionless time) to the gas phase, respectively, by the heat conduction, the convection, the heat transfer between the two phases, and the combustion heat release. CD_p, $-SD$ and *RH* are the energy inputs to the particulate phase, respectively, by the heat conduction, the heat transfer between the two phases, and the radiation. Figure 6 shows the local energy balance in an ordinary premixed gas-phase flame for comparison. In the gas-phase flame, the heat conduction tends to offset the chemical reaction in the exothermic zone and the convection in the preheat zone. In the

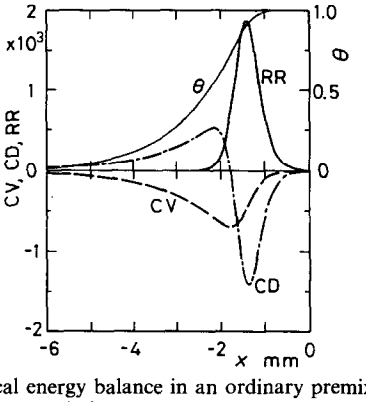

FIG. 6. Local energy balance in an ordinary premixed gas-phase flame (this flame is used as the reference state).

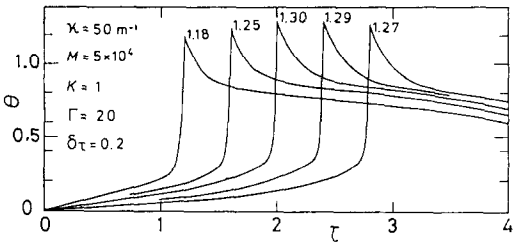

FIG. 7. Temperature profiles in the gas phase for several positions of the reaction zone ($\kappa = 50$ m^{-1}, $\tau_e = 4$, $\tau_f/\tau_e = 0.3$–0.7).

present two-phase case, the heat transfer to the solid phase has a role comparable with heat conduction in the local energy balance in the gas phase, and the heat conduction tends to offset the inter-phase heat transfer in the solid phase, as shown in Fig. 5. Outside the vicinity of the exothermic zone, the local energy balance in Fig. 4 shows that the heat transfer between the two phases tends to offset the convection in the gas phase and the radiation in the solid phase, as shown in a previous work [4]. Although the heat conduction in the solid phase is important for the local energy balance in the exothermic zone, its contribution to the excess enthalpy burning is small, since the energy transport is effective for excess enthalpy burning only when it returns energy across the exothermic zone. This energy feedback is executed by the radiative flux, which determines the approximate preheated temperature. The conductive flux modifies the temperature profiles in the vicinity of the exothermic zone. Moreover, the contribution of the solid phase in the exothermic zone reduces the gas-phase temperature and burning velocity, which is shown in Fig. 10.

Comparing this result with ordinary gas-phase flames, the burning velocity and flame thickness are: $S_u/S_{u0} = 5.0$ and $\Delta/\Delta_0 = 0.67$. The flame thickness is defined here as the thickness where the mass production rate exceeds 1/1000 of its maximum. The unburnt mixture would have to have been heated up to 680 K to realize the same gas-phase burning velocity, in which case the flame thickness would have become thinner (0.43) and the maximum temperature would be even higher (1.32 in dimensionless form). Therefore, a detailed examination of the temperature profiles suggests that the porous medium suppresses the maximum flame temperature while it preheats the unburnt mixture.

3.2. *Effects of the position of the reaction zone*

Figures 7–9 show the profiles of the gas-phase temperature, the burning velocity and the flame thickness, and the overall energy balance of the system, respectively. The numerals in Fig. 7 denote the maximum temperatures. They are highest when the reaction zone is near the center of the porous medium. The burning velocity is also maximum under the same conditions as shown in Fig. 8. The maximum temperature and

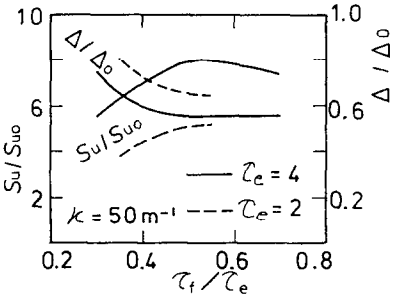

FIG. 8. Effects of the position of reaction zone on burning velocity and flame thickness ($\kappa = 50$ m^{-1}, $\tau_e = 2$ and 4, $\tau_f/\tau_e = 0.3$–0.7).

burning velocity decrease, while the flame thickness increases when the reaction zone is moved upstream, as a result of radiative heat loss from the upstream end, which increases appreciably when the reaction zone moves upstream, as shown in Fig. 9. The steady-state solution could not be obtained when the approximate flame position was assumed close to the upstream end of the porous medium because the radiation heat loss increases abruptly and the mass burning velocity changes appreciably even for a small deviation of profiles.

The computed results also show that the burning velocity decreases when the reaction zone is moved downstream from the center of the porous medium. Considering ordinary gas-phase flames, a flame is unstable when the burning velocity decreases as it is moved downstream. Therefore, the stability of the flames in this region should be clarified in further works. A detailed survey of the computed results shows that the decrease in burning velocity in this region is due to the reduction of the energy feedback across the reaction zone by radiation.

3.3. *Effects of absorption coefficient*

Figure 10 shows the maximum temperature, burning velocity and flame thickness. The absorption coefficient is perhaps the most important property of the porous media. There are many ways to change

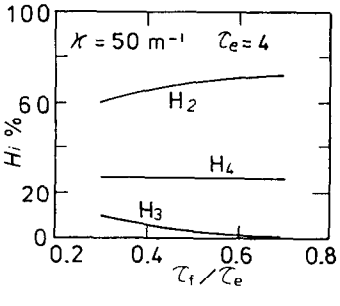

FIG. 9. Effects of the position of the reaction zone on the overall energy balance ($\kappa = 50$ m^{-1}, $\tau_e = 4$, $\tau_f/\tau_e = 0.3$–0.7). H_2, H_3, and H_4, are the exit sensible enthalpy flow, the upstream radiative loss and the downstream radiative loss, respectively, all of which are normalized against the total heat release rate.

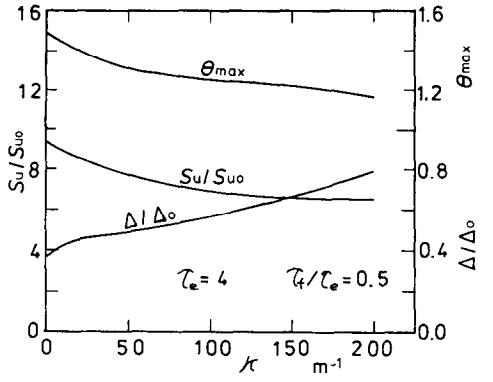

FIG. 10. Effects of absorption coefficient on maximum temperature, burning velocity and flame thickness (κ = 0–200 m^{-1}, $\tau_e = 4$, $\tau_f/\tau_e = 0.50$).

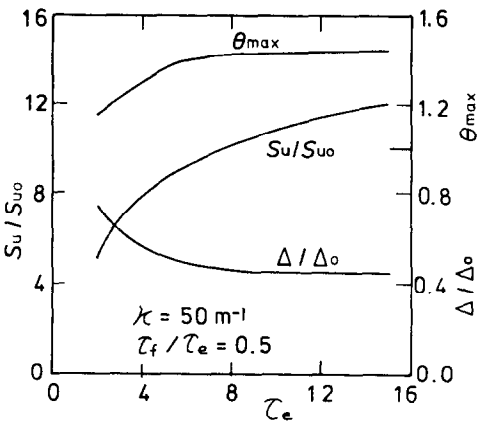

FIG. 11. Effects of total optical thickness on maximum temperature, burning velocity and flame thickness (κ = 50 m^{-1}, τ_e = 2–15, $\tau_f/\tau_e = 0.50$).

the absorption coefficient in a practical system. Such changes, however, are usually accompanied by variations of other properties. Although the porous medium is assumed to be made up of dispersed fine solid particles in this study, spongy metals and spongy ceramics are handy materials for the porous medium in a practical system, and it is easiest to change the absorption coefficient by changing its void fraction, which is equivalent to changing the number density of the particles in the analytical model. Therefore, all the dimensionless variables and parameters including the number density were changed in the computations while the particle sizes remained constant. An increase in absorption coefficient causes not only an increase in the optical thickness of the reaction zone, but also an increase in the surface area of particles leading to an increasing role of the inter-phase heat transfer and an accompanying decrease of the maximum temperature and burning velocity, and increased thickness of the reaction zone. Since the optical thickness of the porous medium is fixed, as shown in Fig. 10, an increase in absorption coefficient corresponds to a decrease in the geometrical thickness. Therefore, the normalized reaction zone thickness in the porous medium enlarges rapidly together with the absorption coefficient. The heat losses from both ends of the porous medium also increase together with the absorption coefficient. In the course of computation, the increase in the absorption coefficient requires more computational mesh points and more computational time.

The limit of the optically sparse porous medium is $\kappa = 0$, which corresponds to combustion in a radiative heat exchanger composed of two separated porous media. The sensible enthalpy of burnt gas is converted into thermal radiation in the downstream porous medium, while the reverse process occurs in the upstream porous medium, and the preheated mixture burns between them. Since the optically sparse limit merely denies the contribution of radiation inside the reaction zone and the preheat temperature is controlled by the total optical length, the analyses with a differential formulation of radiation in a semi-infinite system cannot give a correct scheme of a radiation controlled flame.

3.4. *Effects of total optical thickness*

Figure 8 shows the comparison between $\tau_e = 2$ and 4. The burning velocity for the thicker medium is far larger and the thickness of the reaction zone is thinner than that for the thinner medium. The temperatures in Fig. 7 are also higher than those in Fig. 2. These results can be attributed to the decrease in the heat loss from the upstream end with increased total optical thickness. Calculations were executed for τ_e up to 15 and the results are shown in Figs. 11 and 12 for the cases for which the reaction zone is at the center of each porous medium. Figure 11 shows a monotonic increase in maximum temperature and burning velocity and a monotonic decrease in reaction zone thickness with total optical thickness, although the effects become small for optical thicknesses greater than 8. Since the accuracy of the calculated divergence of the radiative heat flux worsened, computation was not

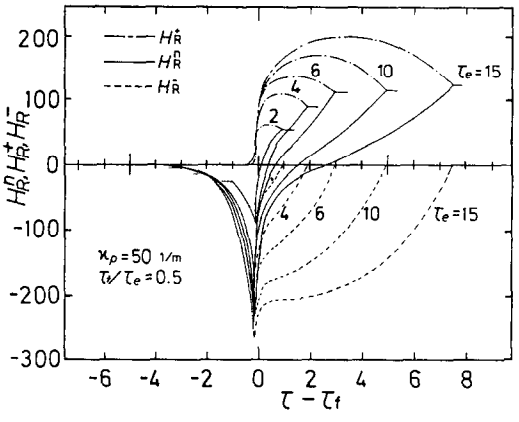

FIG. 12. Effects of total optical thickness on profiles of the radiant fluxes in the porous medium (κ = 50 m^{-1}, τ_e = 2–15, $\tau_f/\tau_e = 0.50$).

executed for larger optical thicknesses. However, it is surmized that the burning velocity would not increase much even if the optical thickness increased further because the maximum temperature seems to have approached an asymptote and because the contribution of radiation decreases with flow rate if the temperature profile does not change appreciably [4]. Figure 12 shows that the upstream radiation heat loss becomes negligible when the optical thickness is larger than 8.

4. CONCLUDING REMARKS

Based on a strict treatment of radiation, a detailed numerical analysis has been performed for a one-dimensional model of premixed combustion in a porous medium. The results revealed by this study are summarized below.

(1) It is shown that the thermal structures (profiles of temperature, radiant energy density, etc.) in a porous medium depend strongly on the absorption coefficient and total optical thickness of the porous medium, as well as on the position of the reaction zone within the porous medium. The effects of these parameters on the flame structures and burning velocity have been elucidated.

(2) The disclosed thermal structures show a strong energy feedback across the reaction zone causing excess enthalpy burning.

(3) The local and total energy balances of the system have been revealed, and the importance of radiation heat transfer has been demonstrated.

REFERENCES

1. R. Echigo, Effective energy conversion method between gas enthalpy and thermal radiation and application to industrial furnaces, *Proceedings of the 7th International Heat Transfer Conference*, Munich, Vol. VI, pp. 361–366 (1982).
2. R. Echigo, M. Kurusu, K. Ichimiya and Y. Yoshizawa, Combustion augmentation of extremely low calorific gases (application of the effective energy conversion method from gas enthalpy to thermal radiation), *Proceedings of the 1983 ASME/JSME Thermal Engineering Joint Conference*, Honolulu, Vol. IV, pp. 99–103 (1983).
3. R. Echigo, K. Hanamura, Y. Yoshizawa and T. Tomimura, Radiative heat transfer enhancement to a water tube by combustion gases in porous media, *Proceedings of International Symposium on Heat Transfer*, Beijing, Vol. 3, pp. 186–193 (1985).
4. R. Echigo, Y. Yoshizawa, K. Hanamura and T. Tomimura, Analytical and experimental studies on radiative propagation in porous media with internal heat generation, *Proceedings of the 8th International Heat Transfer Conference*, San Francisco, Vol. II, pp. 827–832 (1986).
5. L. D. Smoot, Pulverized coal diffusion flames; a perspective through modeling, Eighteenth Symposium (International) on Combustion, The Combustion Institute, pp. 1185–1202 (1981).
6. J. de Ris, Fire radiation; a review, Seventeenth Symposium (International) on Combustion, The Combustion Institute, pp. 1003–1016 (1979).
7. N. Selcuk, R. G. Siddall and J. M. Beer, A comparison of mathematical models of the radiative behaviour of a large-scale experimental furnace, Sixteenth Symposium (International) on Combustion, The Combustion Institute, pp. 53–62 (1977).
8. W. Arpaci and R. J. Tabaczynski, Radiation-affected laminar flame propagation, *Combustion Flame* **46,** 315–322 (1982).
9. G. Joulin and B. Deshaies, On radiation-affected flame propagation in gaseous mixtures seeded with inert particles, *Combust. Sci. Technol.* **47,** 299–315 (1986).
10. W. W. Yuen and S. H. Zhu, The effect of thermal radiation on the propagation of laminar flames, *Proceedings of the 8th International Heat Transfer Conference*, San Francisco, Vol. II, pp. 833–841 (1986).
11. F. J. Weinberg, Combustion temperatures: the future?, *Nature* **233**(5317), 239–241 (1971).
12. T. Takeno and K. Hase, Effects of solid length and heat loss on an excess enthalpy flame, *Combust. Sci. Technol.* **31,** 207–215 (1983) and works cited.
13. Y. Kotani, H. F. Behbahani and T. Takeno, An excess enthalpy flame combustor for extended flow ranges, Twentieth Symposium (International) on Combustion, The Combustion Institute, pp. 2025–2033 (1984).
14. (For example) F. A. Williams, *Combustion Theory*. Addison–Wesley, Reading, Massachusetts (1965).
15. K. Y. Wang and C. L. Tien, Thermal insulation in flow systems: combined radiation and convection through a porous segment, *Trans. ASME J. Heat Transfer* **106**(2), 453–459 (1984).
16. D. B. Spalding, The theory of flame phenomena with a chain reaction, *Phil. Trans. R. Soc. London* **249A,** 1–25 (1956).

ETUDE ANALYTIQUE DE LA STRUCTURE DE FLAMME CONTROLEE PAR RAYONNEMENT

Résumé—Cette étude est entreprise pour clarifier les effets du transfert radiatif sur la structure de la flamme et la vitesse de combustion dans des systèmes diphasiques gaz–solide. Basée sur un traitement rigoureux du rayonnement, une analyse numérique détaillée est conduite pour un modèle monodimensionnel de combustion prémélangée dans un milieu poreux, et les effets du coefficient d'absorption et de l'épaisseur optique totale du milieu poreux aussi bien que de la position de la zone de réaction sont étudiés vis-à-vis des structures de la flamme et de la vitesse de combustion.

ANALYTISCHE UNTERSUCHUNG DER STRAHLUNGSSTRUKTUR EINER GEREGELTEN FLAMME

Zusammenfassung—Ziel der Untersuchung war die Klärung des Einflusses der Strahlungswärmeübertragung auf die Flammenstruktur und die Brenngeschwindigkeit in gasförmig-festen Zwei-Phasen-Systemen. Es wurde eine detaillierte numerische Analyse für ein eindimensionales Modell einer vorgemischten Verbrennung in einem porösen Medium durchgeführt. Außerdem wurden die Einflüsse des Absorptionskoeffizienten und der gesamten optischen Dichte des porösen Mediums sowie der Position der Reaktionszone innerhalb des porösen Mediums bezüglich der Flammenstruktur und der Brenngeschwindigkeit aufgeklärt.

АНАЛИТИЧЕСКОЕ ИССЛЕДОВАНИЕ СТРУКТУРЫ ПЛАМЕНИ С РЕГУЛИРУЕМЫМ ИЗЛУЧЕНИЕМ

Аннотация—Изучается влияние радиационного теплопереноса на структуру пламени и скорость горения в двухфазных системах газ–твердое тело. На основе строгого рассмотрения излчения проведен детальный численный анализ одномерной мойели горения в пористой среде с предварительным смешиванием; выяснено влияние коэффициента поглощения суммарной оптической толщины пористой среды, а также положения зоны реакции в пористой среде на структуры пламени и скорость горения.